

# Comparison of the discounted costs of controlled asynchronous electric drives with matrix and with DC link frequency converters

Viktor Petrushyn<sup>1</sup>, Juriy Plotkin<sup>2</sup>, Vasily Horoshko<sup>1</sup>, Rostyslav Yenoktaiev<sup>2</sup>, Andrii Yakimets<sup>1</sup>

<sup>1</sup>Department of Electromechanical Engineering, Institute of Electrical Engineering and Electromechanics

Odessa Polytechnic National University, Odessa, Ukraine

<sup>2</sup>Berlin School of Economics and Law, Berlin, Germany

## Article Info

### Article history:

Received Apr 25, 2025

Revised Oct 3, 2025

Accepted Oct 17, 2025

### Keywords:

Frequency-controlled

asynchronous drive

Inflation rate

Matrix converter

Operating modes

Ranged discounted costs

Voltage source inverter with

DC link

## ABSTRACT

A quality criterion based on discounted costs is proposed, which demonstrates a significant advantage of the variable frequency asynchronous motor drive with a matrix converter over the drive with a voltage source inverter, which contains a DC link. A MATLAB software simulation was conducted to ascertain the control characteristics. In light of the control range afforded by both drives, a criterion for discounted costs is proposed that is calculated as a mid-range within a specific rotational speed control range, or is determined based on a given tachogram. The aforementioned costs include the expense of the drive, the cost of losses, maintenance costs, amortization charges, and the cost of reactive power compensation due to phase shifts of the main harmonic current and voltage. In this study, we put forth a novel proposal for the incorporation of the cost of distortion power compensation resulting from the presence of harmonic components of the input current. The latter costs characterize the electromagnetic compatibility of the drive with the network. For the first time, a quality criterion for a regulated electric drive is proposed, which has a cost component that takes into account the electromagnetic compatibility of the drive with the network. A significant reduction in this component in a drive with a matrix converter compared to a drive with a DC link predetermines a reduction in discounted costs. For a given payback period and annual inflation rate, it was determined that the mid-range discounted costs were reduced by more than 11 times and the tachogram based discounted costs were reduced by more than 10 times for a drive with a matrix converter in comparison to a drive with a DC link.

*This is an open access article under the [CC BY-SA](https://creativecommons.org/licenses/by-sa/4.0/) license.*



## Corresponding Author:

Viktor Petrushyn

Department of Electromechanical Engineering, Institute of Electrical Engineering and Electromechanics

Odessa Polytechnic National University

Odessa 65044, Ukraine

Email: victor\_petrushin@ukr.net

## 1. INTRODUCTION

Due to the significant advantages of matrix frequency converters (direct conversion of input AC voltage to output AC voltage with specified value and frequency, direct connection between source and load, improved operational characteristics), they are the most promising for frequency-controlled asynchronous electric drives (FCAED) [1]–[4]. As matrix converters improve and become more cost-effective, they have the potential to replace the most widely used converters based on voltage source inverters with a DC link [5], [6]. An important

question is the economic justification for such a replacement. The quality of one or another controlled electric drive can be assessed by various criteria. It is advisable to take into account the specifics of its operation, namely, providing a certain control range. Thus, the criteria should be range-based, providing an assessment of quality at various points in the control range. The simplest approach seems to be determining the mid-range criteria for a given control range that meets the technological task. In some cases, the technological task associated with determining the operational mode of the drive can be represented by specific rotational speed values, which are characterized by a given tachogram. Then, the criteria calculations could be carried out considering this tachogram.

However, the widely used criteria, such as the efficiency coefficient  $\eta$  [7]–[9], or the power factor  $\chi$ , which determines the energy and electromagnetic compatibility of the drive with the power supply network [10], or the criterion based on the product of these coefficients [11], do not fully reflect all the technical and economic aspects that determine quality. For this purpose, a range-based criterion of discounted costs can be used, which includes not only cost indicators related to initial capital investments but also operating costs associated with energy losses, maintenance costs, and amortization charges. This criterion, for example, is widely used in the development of electric machines and crane equipment [12], [13].

For frequency-controlled asynchronous drives, this criterion is range-based [14], and it requires considering not only the costs of compensating reactive power caused by phase shifts of the main harmonic currents and voltages but also the costs of compensating distortion power determined by the presence of harmonic components in the input current of the drive. Such a range-based discounted costs criterion can be determined based on experimental research or operational data [15], as well as by using mathematical modeling of various FCAED systems. One of the most widely used modeling software is MATLAB [16]–[18]. In FCAED models, the components included in the drive are considered collectively, and the mutual influence of each component is taken into account. This study aims to compare the discounted costs of two FCAEDs with different frequency converters: matrix and with a DC link. For this purpose, mathematical modeling of these drives is carried out in the MATLAB environment to obtain control characteristics, i.e., dependencies of certain indicators (active power consumed by the drive, efficiency, shift coefficients, total harmonic distortion (THD), power, and currents consumed by the drive) on the rotational speed in a given range with a specific load characteristic. To determine THD, the harmonic spectrum of the current consumed by the drive is considered. The required components of the discounted costs criterion are determined based on the control characteristics. Along with the component that considers the costs of compensating reactive power caused by phase shifts between the main harmonics of the current and voltage at the input of the drive, it is proposed to calculate the component that considers the costs of compensating distortion power caused by the presence of harmonic components of the current at the input of the drive. For the first time, a quality criterion for a regulated electric drive is proposed, which has a cost component that takes into account the electromagnetic compatibility of the drive with the network. A significant reduction in this component in a drive with a matrix converter compared to a drive with a DC link predetermines a reduction in discounted costs. The load mode of the considered FCAEDs affects the values of the discounted costs. They also depend on the inflation rate and electromagnetic compatibility requirements. A significant reduction in the discounted costs criterion for the drive with a matrix converter compared to the drive with a DC link converter is confirmed.

## 2. MATHEMATICAL MODELS OF FCAED IMPLEMENTED IN MATLAB SIMULINK

The simulation model of FCAED based on a DC link converter in the MATLAB/Simulink environment is shown in Figure 1. This basic model consists of seven main blocks. The first block is an ideal three-phase power supply source with a line voltage of 380 V and a frequency of 50 Hz. Next, the three-phase voltage is converted to DC using a three-phase diode bridge, and an autonomous voltage inverter with a PWM generator forms the voltage with a specified amplitude and frequency. The capacitance of one capacitor in the DC link is  $C_f = 5.7$  mF. The carrier frequency of the PWM is 6 kHz. The control is based on the frequency regulation law  $U/f = \text{const}$ .

The generated voltage is supplied to a two-pole squirrel-cage asynchronous motor with a rated power of  $P_n = 90$  kW, a rated line voltage of  $U_n = 380$  V, and a rated frequency of  $f_n = 50$  Hz. The stator's active resistance and inductance are  $R_s = 0.028$   $\Omega$ ,  $L_s = 0.363$  mH. The equivalent parameters for the rotor are  $R_r' = 0.0153$   $\Omega$ ,  $L_r' = 0.528$  mH. The mutual inductance is  $L_m = 0.0183$  H. The motor operates on a load characteristic described by the equation  $M(\omega) = 50 + 0.0182 \cdot \omega^2$ . For simulation, different types and magnitudes of loads can be selected, depending on the specific application of the drive. The differential equations were solved using a variable step size method with the “discrete (no continuous state)” approach. The calculation step size is 2  $\mu$ s. By varying the converter's output frequency from 5 to 50 Hz, the motor rotational speed is regulated from 148 rpm to 1481 rpm. Figure 2 shows the schematic of the drive system based on an asynchronous motor and a matrix converter.

The simulation model of such an FCAED in the MATLAB Simulink environment is shown in Figure 3. This model is similar to the previous one with a DC link converter but consists of five main blocks. The main difference is the semiconductor converter and the transistor control system. Their operating frequency is 6 kHz. The internal structure of these blocks is detailed in [19]. The regulation of rotational speed is based on the law of frequency control  $U/f = \text{const}$ .

The remaining parameters of the model with the matrix converter fully correspond to the model with the DC link converter. The costs of frequency converters with a power of 90 kW can vary depending on the manufacturer and model. It is assumed that the cost of the drive with a DC link converter is 3000 c.u. (1000 c.u. for the induction motor and 2000 c.u. for the frequency converter), and the cost of the drive with the matrix converter to be 21000 c.u. (1000 c.u. for the induction motor and 20000 c.u. for the frequency converter).

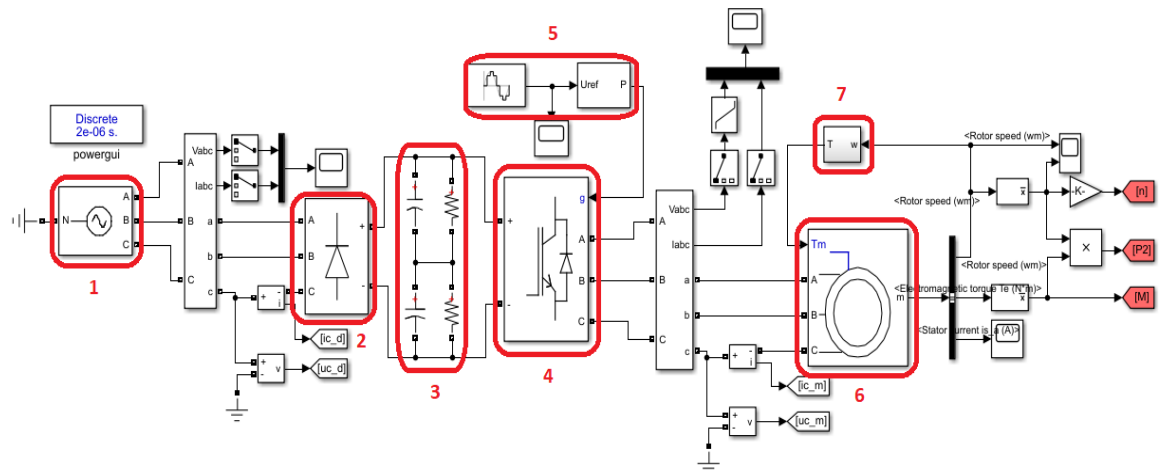


Figure 1. Model of FCAED with a DC link frequency converter: 1) three-phase voltage source, 2) rectifier, 3) filter, 4) autonomous voltage inverter, 5) PWM generator, 6) asynchronous motor, and 7) load

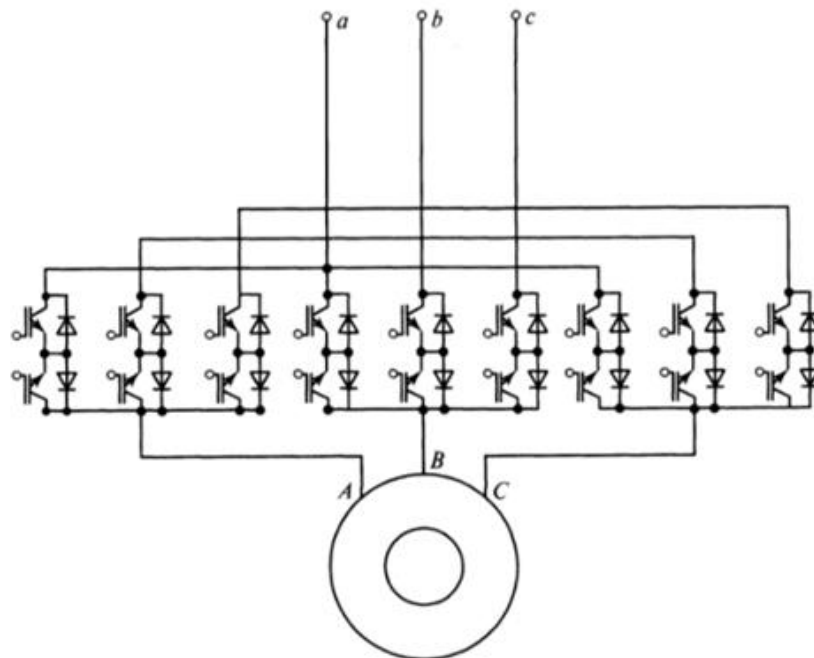


Figure 2. Diagram of FCAED with matrix converter

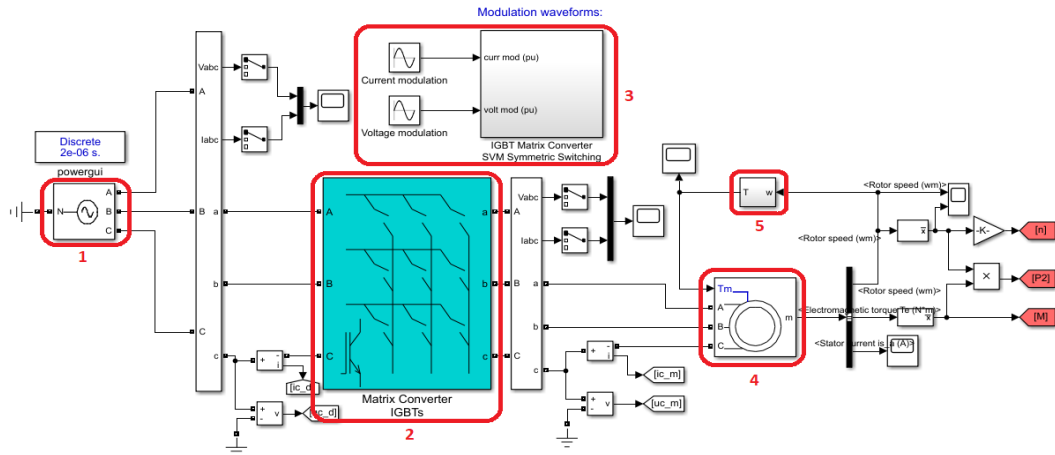


Figure 3. Model of FCAED with matrix frequency converter: 1) three-phase voltage source, 2) matrix semiconductor converter, 3) transistor control system, 4) asynchronous motor, and 5) load

### 3. SIMULATION RESULTS

It is advisable to use MATLAB tools to measure energy indicators, and the solution to such a problem is described in detail in [20]. Energy balance indicators for the fundamental harmonic were considered. The values of the total  $S_1$  (VA) and active  $P_1$  (W) powers made it possible to calculate the phase shift coefficient  $\cos\varphi$ . Using the described modules, the numerical values of the total  $S$  (VA), active  $P$  (W), and non-active  $D$  (VAr) powers are determined using the instantaneous values from voltage and current sensors. The non-active power  $D$  is decomposed into components  $Q_1$  and  $T$ , which are related by the geometric sum  $D^2 = Q_1^2 + T^2$ . Here,  $Q_1$  is the component of the non-active power  $D$  caused by the phase shift of the first harmonic of the current relative to the first harmonic of the voltage, and  $T$  is the distortion power. The power factor of the drive  $\chi_p$  is determined by the power balance considering higher harmonics. It can also be found using the harmonic spectra of the currents and voltages consumed by the drive, determined by THD.

$$\chi = \frac{\cos \varphi}{\sqrt{1 + \text{THD}_U^2 + \text{THD}_I^2 + \text{THD}_U^2 \cdot \text{THD}_I^2}} \quad (1)$$

If we consider a system with an infinite power supply source, where an undistorted three-phase voltage is applied to a distorting load, the expression for the power factor of the electric drive is as (2) [21].

$$\chi = \frac{\cos \varphi}{\sqrt{1 + \text{THD}_I^2}} \quad (2)$$

The power factor can also be expressed through the current distortion factor  $k_I$  and the voltage distortion factor  $k_U$ :

$$\chi = k_U k_I \cos \varphi \quad (3)$$

If the voltage supplied to the drive is sinusoidal, then:

$$\chi = k_I \cos \varphi \quad (4)$$

Calculations of  $\chi$  for the drive are somewhat complex, due to the variable spectrum of higher harmonics, which depends on the regulation parameter and the load magnitude, as well as the converter settings (frequency control law, basic voltage and frequency values of the converter, modulation frequency).

Tables 1-3 present the calculation results of the FCAED with a DC link frequency converter with PWM control, and Tables 4-6 present the FCAED with a matrix converter.  $\text{THD}_U$  and  $k_U$  values are not indicated in Tables 3 and 6, since for an infinite power supply network, they are 0 and 1, respectively. Tables 2 and 4 provide the values of rotational speeds, load torques, and shaft powers. Using the latter, the efficiency of the drives was calculated (Tables 3 and 6).

MATLAB allows obtaining the power factor from the power balance or finding it using the values of  $\text{THD}_I$  (or  $k_I$ ) and  $\cos\varphi$ . Comparison of power factor values determined using MATLAB shows their exceptional

closeness (the difference between  $\chi_p$  and  $\chi$  is observed only in the third decimal place). Oscillography of voltages and currents at the input of the FCAED was performed (Figure 4), and the oscillograms were decomposed into a Fourier series (Figures 5 and 6). As a result, the THD and distortion factors were determined. The oscillograms are shown for an input current of 30.68 A (DC link converter scheme) and an input current of 20 A (matrix converter scheme), and correspond to an input frequency of 25 Hz. Input voltage value 218.3 V.

Table 1. Simulation results with a DC link converter

| f (Hz) | U (V) | I (A)  | U <sub>i</sub> (V) | I <sub>i</sub> (A) | P <sub>i</sub> (W) | S <sub>i</sub> (VA) |
|--------|-------|--------|--------------------|--------------------|--------------------|---------------------|
| 5      | 218.3 | 2.96   | 218.3              | 1.58               | 1032               | 1033.2              |
| 10     | 218.3 | 6.29   | 218.3              | 3.5                | 2282.8             | 2289.9              |
| 15     | 218.3 | 11.55  | 218.3              | 6.73               | 4379.8             | 4406.9              |
| 20     | 218.3 | 19.78  | 218.3              | 12.2               | 7890.6             | 7963.2              |
| 25     | 218.3 | 30.68  | 218.3              | 19.9               | 12854              | 13027               |
| 30     | 218.3 | 45.4   | 218.3              | 31.2               | 20046              | 20417               |
| 35     | 218.3 | 64.19  | 218.3              | 46.6               | 29872              | 30546               |
| 40     | 218.3 | 86.13  | 218.3              | 66.2               | 42243              | 43343               |
| 45     | 218.3 | 113.41 | 218.3              | 91.9               | 58654              | 60197               |
| 50     | 218.3 | 143.65 | 218.3              | 122.3              | 78293              | 80066               |

Table 2. Simulation results with a DC link converter

| f (Hz) | P (W)  | D (Var) | S (VA) | n (rpm) | M (N·m) | P <sub>2</sub> (W) |
|--------|--------|---------|--------|---------|---------|--------------------|
| 5      | 1032   | 1639.8  | 1937.5 | 147.7   | 54.4    | 841                |
| 10     | 2282.8 | 3428.8  | 4119.2 | 297.5   | 67.7    | 2109               |
| 15     | 4379.8 | 6166.2  | 7563.4 | 446.6   | 89.9    | 4203               |
| 20     | 7890.6 | 10271   | 12952  | 595.5   | 120.9   | 7541               |
| 25     | 12854  | 15439   | 20090  | 743.9   | 160.7   | 12518              |
| 30     | 20046  | 21959   | 29732  | 892.6   | 209.4   | 19577              |
| 35     | 29872  | 29572   | 42034  | 1039.2  | 265.8   | 28927              |
| 40     | 42243  | 37373   | 56402  | 1186.5  | 331.1   | 41134              |
| 45     | 58654  | 45555   | 74267  | 1332.7  | 404.7   | 56478              |
| 50     | 78293  | 52149   | 94071  | 1479.1  | 487.6   | 75521              |

Table 3. Simulation results with a DC converter

| f (Hz) | cosφ (r.u.) | THD <sub>i</sub> (r.u.) | k <sub>i</sub> (r.u.) | χ <sub>p</sub> (r.u.) | χ (r.u.) | η (r.u.) |
|--------|-------------|-------------------------|-----------------------|-----------------------|----------|----------|
| 5      | 0.999       | 1.586                   | 0.534                 | 0.5326                | 0.5334   | 0.815    |
| 10     | 0.997       | 1.495                   | 0.557                 | 0.5542                | 0.5551   | 0.924    |
| 15     | 0.994       | 1.395                   | 0.583                 | 0.5791                | 0.5791   | 0.96     |
| 20     | 0.991       | 1.283                   | 0.613                 | 0.6092                | 0.6074   | 0.956    |
| 25     | 0.987       | 1.174                   | 0.648                 | 0.6399                | 0.6395   | 0.974    |
| 30     | 0.982       | 1.058                   | 0.688                 | 0.6742                | 0.6752   | 0.977    |
| 35     | 0.978       | 0.945                   | 0.727                 | 0.7107                | 0.7106   | 0.968    |
| 40     | 0.975       | 0.832                   | 0.769                 | 0.749                 | 0.7496   | 0.974    |
| 45     | 0.974       | 0.722                   | 0.811                 | 0.7898                | 0.7906   | 0.963    |
| 50     | 0.978       | 0.617                   | 0.851                 | 0.8323                | 0.8323   | 0.965    |

Table 4. Simulation results with a matrix converter

| f (Hz) | U (V) | I (A)  | U <sub>i</sub> (V) | I <sub>i</sub> (A) | P <sub>i</sub> (W) | S <sub>i</sub> (VA) |
|--------|-------|--------|--------------------|--------------------|--------------------|---------------------|
| 5      | 218.3 | 1.75   | 218.3              | 1.7                | 1111.9             | 1113.1              |
| 10     | 218.3 | 3.7    | 218.3              | 3.63               | 2366.9             | 2374                |
| 15     | 218.3 | 6.84   | 218.3              | 6.68               | 4359.9             | 4373.6              |
| 20     | 218.3 | 12.02  | 218.3              | 11.76              | 7663               | 7697.4              |
| 25     | 218.3 | 20.02  | 218.3              | 19.69              | 12842.7            | 12895.4             |
| 30     | 218.3 | 30.64  | 218.3              | 30.24              | 19732.4            | 19803.6             |
| 35     | 218.3 | 46.73  | 218.3              | 46.35              | 30271.4            | 30352               |
| 40     | 218.3 | 65.25  | 218.3              | 64.83              | 42330.6            | 42451.6             |
| 45     | 218.3 | 89.98  | 218.3              | 89.51              | 58436.4            | 58609.1             |
| 50     | 218.3 | 119.21 | 218.3              | 119.15             | 77924.9            | 78026.6             |

Table 5. Simulation results drive with a matrix converter

| f (Hz) | P (W) | D (Var) | S (VA) | n (rpm) | M (N·m) | P <sub>2</sub> (W) |
|--------|-------|---------|--------|---------|---------|--------------------|
| 5      | 1112  | 279.2   | 1146   | 148.1   | 54.4    | 844                |
| 10     | 2367  | 523.8   | 2424   | 297.7   | 67.7    | 2112               |
| 15     | 4360  | 1015    | 4477   | 447.3   | 90      | 4217               |
| 20     | 7663  | 1784    | 7868   | 596.2   | 121.1   | 7562               |
| 25     | 12843 | 2644    | 13112  | 744.9   | 161.1   | 12564              |
| 30     | 19732 | 3626    | 20063  | 893.4   | 209.7   | 19622              |
| 35     | 30271 | 4473    | 30601  | 1042    | 266.4   | 29075              |
| 40     | 42331 | 5823    | 42730  | 1189    | 332.3   | 41368              |
| 45     | 58436 | 7185    | 58882  | 1338    | 408.3   | 57220              |
| 50     | 77925 | 4697    | 78066  | 1482    | 489     | 75871              |

Table 6. Simulation results with a matrix converter

| f (Hz) | cosφ (r.u.) | THD <sub>i</sub> (r.u.) | k <sub>i</sub> (r.u.) | χ <sub>p</sub> (r.u.) | χ (r.u.) | η (r.u.) |
|--------|-------------|-------------------------|-----------------------|-----------------------|----------|----------|
| 5      | 0.998       | 0.244                   | 0.967                 | 0.9698                | 0.9656   | 0.759    |
| 10     | 0.997       | 0.206                   | 0.976                 | 0.9763                | 0.9732   | 0.892    |
| 15     | 0.997       | 0.218                   | 0.978                 | 0.9739                | 0.975    | 0.967    |
| 20     | 0.995       | 0.211                   | 0.979                 | 0.9739                | 0.9746   | 0.987    |
| 25     | 0.996       | 0.184                   | 0.984                 | 0.9795                | 0.9799   | 0.978    |
| 30     | 0.996       | 0.161                   | 0.988                 | 0.9835                | 0.9844   | 0.994    |
| 35     | 0.997       | 0.128                   | 0.991                 | 0.9892                | 0.9888   | 0.96     |
| 40     | 0.997       | 0.113                   | 0.993                 | 0.9906                | 0.9903   | 0.977    |
| 45     | 0.997       | 0.092                   | 0.995                 | 0.9924                | 0.9925   | 0.979    |
| 50     | 0.999       | 0.032                   | 0.999                 | 0.9982                | 0.9982   | 0.974    |

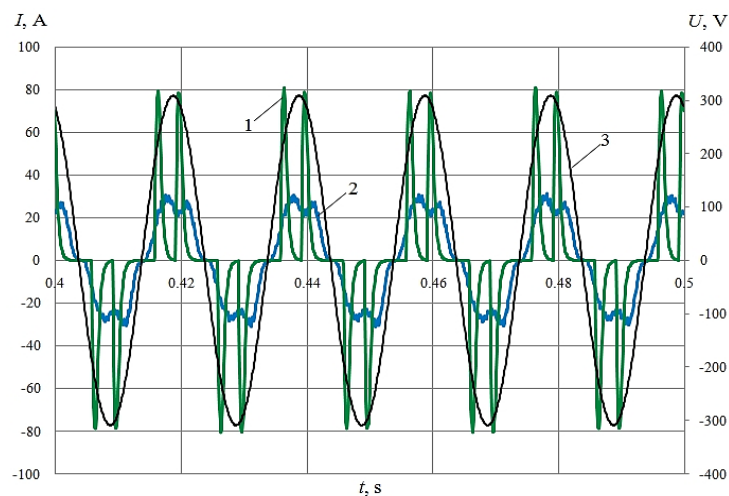


Figure 4. Oscillograms of voltage and currents at the input of the converter: 1) current of the FCAED with a DC link frequency converter, 2) current of the FCAED with a matrix converter, and 3) voltage

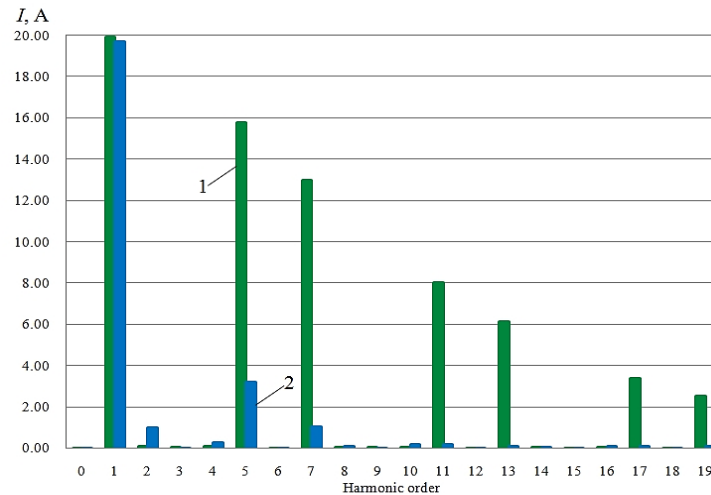


Figure 5. Current decomposition into a Fourier series: 1) a scheme with a DC link converter and 2) a scheme with a matrix converter

The harmonic composition of the current changes significantly when using a matrix converter. The reduction of higher harmonic components leads to an increase in the power factor. Figure 6 shows the family of mechanical characteristics (for different regulation parameters  $KF = f/f_n$ ) of the asynchronous motor 4A250M4 and the fan-type load characteristic.

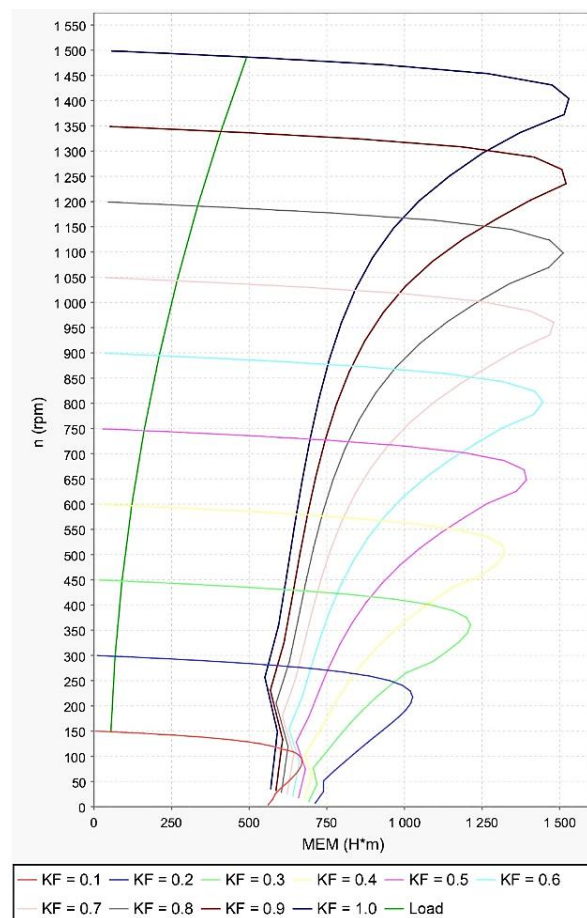


Figure 6. Family of mechanical characteristics and load characteristics

The obtained simulation results allowed the construction of the following control characteristics (Figures 7-11): currents consumed by the drives, active power consumed by the drives, drive efficiency, power factor, phase shift, and THD coefficients. The effective values of currents consumed by the FCAD are lower when using the matrix converter. The active power consumed by the drives with different frequency converters is almost identical across the entire control range. In the initial part of the control range, the efficiency of the drive with the matrix converter is slightly lower than the efficiency of the drive with the DC link converter. Further along, the efficiency values become comparable.

Throughout the entire control range, the phase shift coefficients are practically identical and close to 1 for the two considered cases of FCAED. The power factor of the FCAED with a DC link frequency converter is significantly lower than the power factor of the FCAED with a matrix converter at the beginning of the control range and increases, approaching the power factor of the matrix converter, at the end of the control range. With an increase in the number of revolutions, THD<sub>i</sub> decreases, and there is a convergence of their values for the two FCAED.

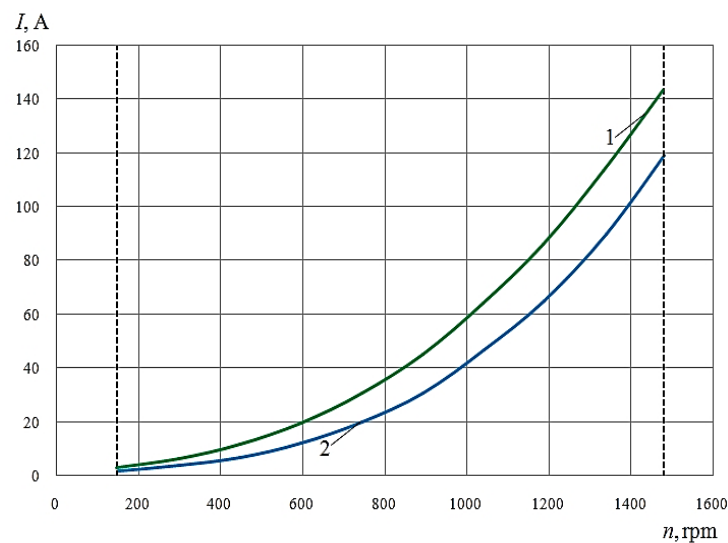


Figure 7. Control characteristics of currents consumed by the drives: 1) DC link converter scheme and 2) matrix converter scheme

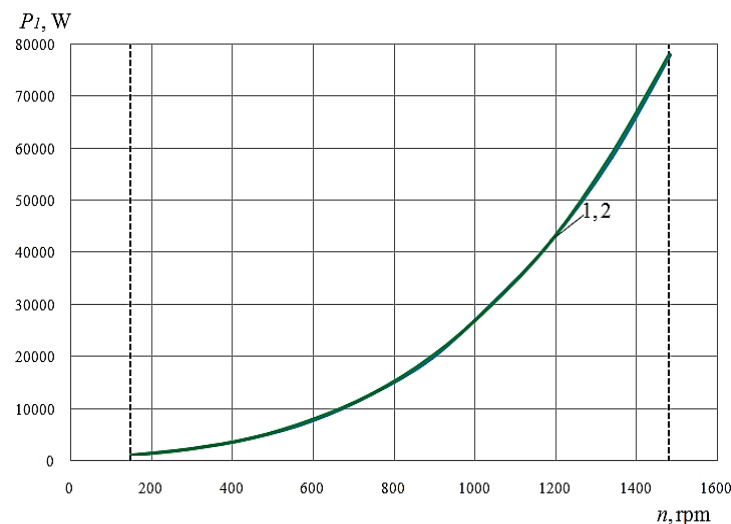


Figure 8. Control characteristics of active power consumed by the drives: 1) DC link converter scheme and 2) matrix converter scheme

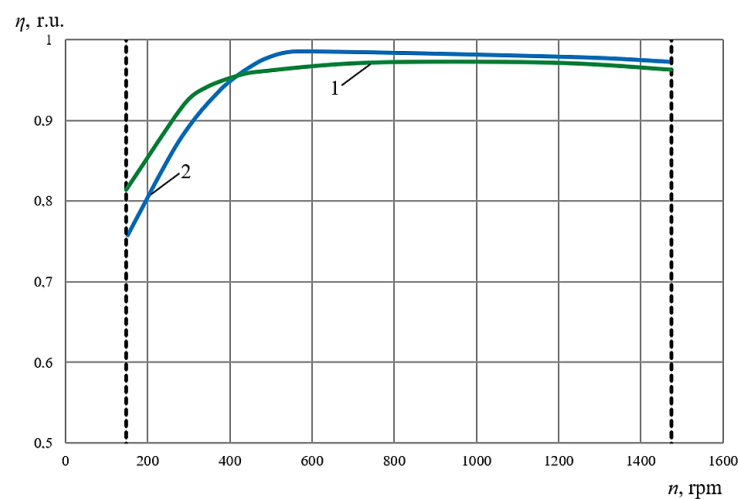


Figure 9. Control characteristics of drive efficiency: 1) DC link converter scheme and 2) matrix converter scheme

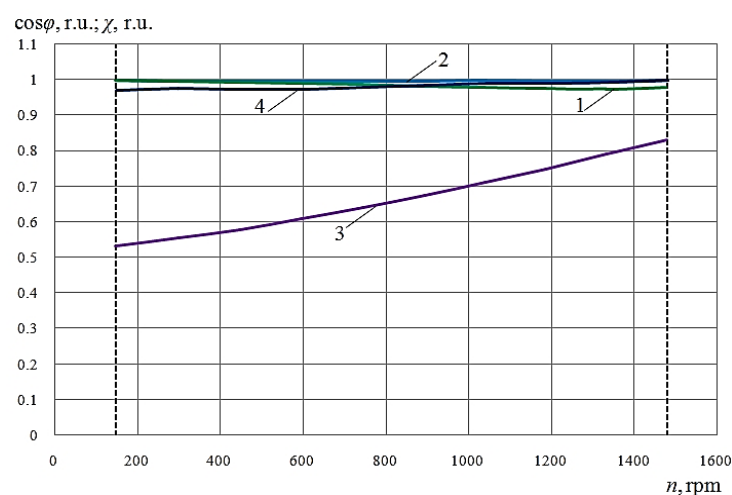


Figure 10. Control characteristics of phase shift coefficients: 1) DC link converter scheme, 2) matrix converter scheme, and power factor coefficients, 3) DC link converter scheme, and 4) matrix converter scheme

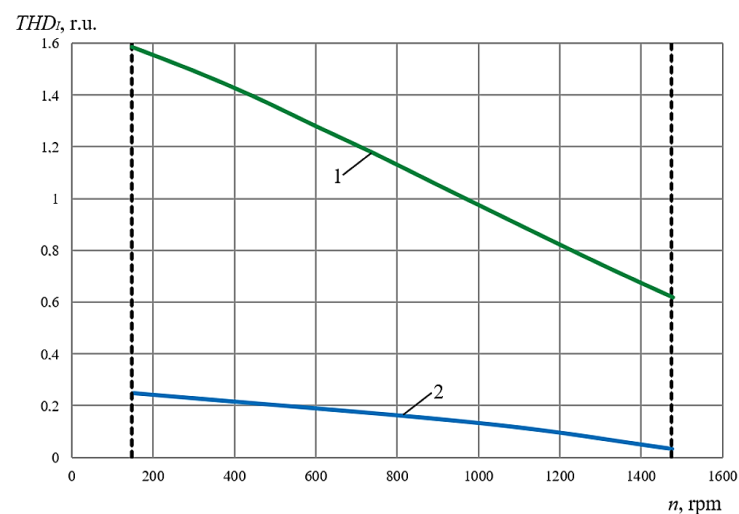


Figure 11. Controlled characteristics of  $THD_1$  for drives: 1) scheme with a DC link converter and 2) scheme with a matrix converter



#### 4. CALCULATION OF THE RANGE CRITERION OF DISCOUNTED COSTS

According to [22], the reactive power  $Q_1$  and the distortion power  $T$  for a known active power  $P_1$ , consumed by the drive, are determined:

$$Q_1 = P_1 \cdot \operatorname{tg} \varphi, \quad T = P_1 \cdot \sqrt{\operatorname{tg}^2 \chi - \operatorname{tg}^2 \varphi} \quad (5)$$

Values of various criteria depend on the operating mode of the load. Simple criteria, such as efficiency and power factor of the drive, and complex criteria, characterized by dependencies on several simple criteria, can be considered.

It is also proposed that when calculating the required criteria, the operating time at each rotational frequency within the control range should be taken into account, determined by the technological requirements of the drive load. Thus, a time diagram of the load operation, i.e., a tachogram, must be specified. In this case, the calculation of ranged criteria is performed considering the duration of the motor's operation at each specified point within the control range according to (6):

$$\eta_{dt} = \frac{\sum_i (\eta(n_i) \cdot t_{n_i})}{\sum_i t_{n_i}}, \quad \chi_{dt} = \frac{\sum_i (\chi(n_i) \cdot t_{n_i})}{\sum_i t_{n_i}}, \quad \cos \varphi_{dt} = \frac{\sum_i (\cos \varphi(n_i) \cdot t_{n_i})}{\sum_i t_{n_i}} \quad (6)$$

where  $t_{n_i}$  is the operating time of the motor at the rotational speed  $n_i$ , where  $i$  is the ordinal number of the tachogram segment.

To minimize energy losses across the entire control range from  $n_1$  to  $n_2$  [23], a mid-range efficiency criterion is required:

$$\eta_{cd} = \frac{1}{n_2 - n_1} \cdot \int_{n_1}^{n_2} \eta(n_i) \, dn \quad (7)$$

Mid-ranged criteria for power factors (minimization of reactive power consumption and distortion power), phase shift between the fundamental voltage harmonics and the current consumed by the drive (minimization of reactive power consumption) can also be utilized:

$$\chi_{cd} = \frac{1}{n_2 - n_1} \cdot \int_{n_1}^{n_2} \chi(n_i) \, dn, \quad \cos \varphi_{cd} = \frac{1}{n_2 - n_1} \cdot \int_{n_1}^{n_2} \cos \varphi(n_i) \, dn \quad (8)$$

A complex criterion that takes into account both manufacturing and operating costs of the drive and is based on several simple criteria is the criterion of discounted costs (DDC). To determine it, it is necessary to calculate the drive's consumed active power, either mid-range or range-based, based on the control characteristics  $P_1 = f(n)$ , considering the specified tachogram of the drive operation:

$$P_{1cd} = \frac{1}{n_2 - n_1} \cdot \int_{n_1}^{n_2} P_1(n_i) \, dn, \quad P_{1dt} = \frac{\sum_i (P_1(n_i) \cdot t_{n_i})}{\sum_i t_{n_i}} \quad (9)$$

Then the expressions for calculating DDC, which can also be average-range or range-based, considering the specified tachogram of the drive operation, are as follows:

$$DCC_{cd} = \frac{1}{n_1 - n_2} \cdot \int_{n_1}^{n_2} DCC(n_i) \, dn; \quad DCC_{dt} = \frac{\sum_i (DCC(n_i) \cdot t_{n_i})}{\sum_i t_{n_i}} \quad (10)$$

The DCC criterion of an electric drive should consider the influence on the inflation criterion [24]. This is related to the relatively long (5-8 years) normative payback periods of frequency-controlled electric drives. If inflation is not considered, then with the known total cost of the drive  $CED$ , the criterion value is determined as (11):

$$DCC = (CED + C_{rpc1} + C_{rpc2}) \cdot [1 + (k_d + k_s)] + C_L \quad (11)$$

where  $C_{rpc1}$  is the cost of reactive power compensation, in conventional units (c.u.);  $C_{rpc2}$  is the cost of distortion power compensation, in conventional units (c.u.);  $C_L$  is the annual cost of energy losses, in conventional units (c.u.);  $k_d$  is the share of costs for depreciation charges;  $k_s$  is the share of maintenance costs during the operation of the drive. For FCAED, the values of  $k_d = 0.065$ ,  $k_s = 0.069$  are taken to be the same as for general industrial AM.

The expressions  $C_{rpc1}$  and  $C_{rpc2}$  for a known control range are as (12):

$$C_{rpc1} = c_{k1} \cdot k_{my} \cdot P_{1cd} \cdot [\operatorname{tg}(\arccos \varphi_{cd}) - \operatorname{tg} \varphi_0] \cdot t_{ED} \quad (12)$$

where  $c_{k1}$  is the cost for 1 kVAr reactive power compensating devices installation (in the following calculations it is taken equal to 10 c.u.);  $C_{rpc1}$  is the cost of installing 1 kVAr reactive power compensation devices (in subsequent calculations assumed to be 10 c.u.),  $k_{my}$  is the participation factor of FCAED in load peaks (in subsequent calculations assumed to be 0.25);  $\varphi$  is the phase angle between the current and voltage of the FCAED, at which reactive power compensation is not required (in subsequent calculations assumed  $\operatorname{tg} \varphi_0 = 0.484$ ). The proposed component  $C_{rpc2}$ , for the first time, allows for the consideration of costs associated with distortion power compensation by electromagnetic compatibility requirements determined by THD:

$$C_{rpc2} = c_{k2} \cdot k_{my} \cdot P_{1cd} \cdot \left\{ \sqrt{[\operatorname{tg}(\arccos \chi_{cd})]^2 - [\operatorname{tg}(\arccos \varphi_{cd})]^2} - \operatorname{tg} \left[ \arccos \left( \frac{1}{\sqrt{1 + \operatorname{THD}_{ID}^2 + \operatorname{THD}_{UD}^2 + \operatorname{THD}_{ID}^2 \cdot \operatorname{THD}_{UD}^2}} \right) \right] \right\} \cdot t_{ED} \quad (13)$$

Where  $c_{k2}$  is the cost of installing 1 kVAr of distortion power compensating devices (in subsequent calculations taken as 20 conventional units). In mechatronic systems powered by an infinite power network, due to the sinusoidal nature of the supply voltage,  $\operatorname{THD}_U$  can be considered zero and excluded from (13).

Standards [25], [26] define the permissible values for the coefficients of total harmonic current distortion  $\operatorname{THD}_{ID}$ . In the expression for the cost of active power losses per year with a known time diagram of drive operation, the (14) are used:

$$C_L = c_{ae} \cdot P_{1cd} \cdot (1 + a_r - \eta_{cd}) \cdot t_{ED} \quad (14)$$

where  $c_{ae}$  is the cost of 1 kWh of active energy (in subsequent calculations taken as 1 conventional unit);  $a_r$  is the coefficient accounting for losses in distribution networks (in subsequent calculations taken as 0.04);  $t_{ED}$  is the duration of drive operation during the year (in subsequent calculations taken as 2000 hours). When the time diagram of motor operation is determined, the range values of the present value components  $C_{rpc1}$ ,  $C_{rpc2}$ , and  $C_L$  are calculated using:  $\eta_{dt}$ ,  $\chi_{dt}$ ,  $\cos \varphi_{dt}$ ,  $P_{1dt}$ .

The expression of the considered criterion for the given cost of FCAED can also be presented in general form as (15):

$$DCC = K + \sum_{i=1 \dots T_n} Y_i \quad (15)$$

where  $K = c_{ep} + C_{rpc1} + C_{rpc2}$  are the initial capital investments, and  $Y_i = (k_d + k_s) \cdot (c_{ep} + C_{rpc1} + C_{rpc2}) + C_L$  are the annual expenses.

If inflation is not taken into account, the amount of annual expenses is constant  $Y_i = \text{const}$ , and equal to the calculated value, determined for the first year of operation. The expression for the given costs to account for annual inflation is transformed into the form:

$$DCC = K + Y_1 \cdot \frac{1 + (1 + d_{INF1}) + (1 + d_{INF1})(1 + d_{INF2}) + (1 + d_{INF1}) \dots (1 + d_{INF(T_n-1)})}{T_n} \quad (16)$$

where  $d_{INF1}$ ,  $d_{INF2}$ , and  $d_{INF3}$  are the projected inflation values for the current years within the payback period  $T_n$ .

If, for the sake of simplicity, an average annual inflation rate  $d_{INF1}$ , is set for the payback period, then the inflation factor is calculated as (17):

$$k_{INF} = \frac{\sum_{m=0}^{T_n-1} \left(1 + \frac{d_{INF}}{100\%}\right)^m}{T_n} \quad (17)$$

where  $d_{INF}$  is the average annual inflation rate (in %).

Two operating modes are considered. In one mode, the drive operates in the speed range of 148-1479 rpm, and for this range, the average values of the coefficients and the active power consumed by

the FCAED are determined. In the second mode, the drive operates according to the following tachogram: 400 s at 300 rpm, 600 s at 600 rpm, 600 s at 1479 rpm. The coefficients and active power consumption are calculated according to the respective expressions. It should be noted that in this case, reactive power compensation can be disregarded since  $\tan \varphi_0$  is significantly less than 0.484. Assuming an average inflation rate of 5.3% and a payback period of 5 years, the inflation factor  $k_{INF}$  will be 1.112. In subsequent calculations, a permissible total harmonic current distortion coefficient  $THD_{ID} = 10\%$  was used. The calculation results are presented in Table 7. Similar calculations for the indicators of FCAEDs with a matrix converter have been performed (Table 8). In this case, the inflation coefficient  $THD_{ID} = 10\%$ .

Table 7. Indicators of a drive with a DC link frequency converter

| Parameters              | Range is set | Tachogram is set | Drive                                      |  |
|-------------------------|--------------|------------------|--|--|
|                         |              |                  | Range is set taking into account inflation | Tachogram is set taking into account inflation |
| $\eta$ , r.u.           | 0.948        | 0.951            | 0.948                                      | 0.951  |
| CED, c.u.               | 3000         | 3000             | 3000                                       | 3000   |
| $\cos \varphi_1$ , r.u. | 0.985        | 0.988            | 0.985                                      | 0.988  |
| P1, kW                  | 25754        | 32890            | 25754                                      | 32890  |
| $\chi$ , r.u.           | 0.667        | 0.679            | 0.667                                      | 0.679  |
| Crpc2, $10^6$ c.u.      | 258.36       | 318.98           | 258.36                                     | 318.98   |
| CL, $10^6$ c.u.         | 4.74         | 5.85             | 4.74                                       | 5.85   |
| K, $10^6$ c.u.          | 258.37       | 318.98           | 258.37                                     | 318.98   |
| Y, $10^6$ c.u.          | 39.36        | 48.6             | 43.77                                      | 54.04  |
| DDC, $10^6$ c.u.        | 297.73       | 367.58           | 302.14                                     | 373.01   |

Table 8. The indicators of a drive with a matrix converter

| Parameters              | Range is set | Tachogram is set | Drive                                      |  |
|-------------------------|--------------|------------------|--|--|
|                         |              |                  | Range is set taking into account inflation | Tachogram is set taking into account inflation |
| $\eta$ , r.u.           | 0.947        | 0.958            | 0.947                                      | 0.658  |
| CED, c.u.               | 21000        | 21000            | 21000                                      | 21000  |
| $\cos \varphi_1$ , r.u. | 0.997        | 0.997            | 0.997                                      | 0.997  |
| P1, kW                  | 25704        | 32687            | 25704                                      | 32687  |
| $\chi$ , r.u.           | 0.983        | 0.981            | 0.983                                      | 0.981  |
| Crpc2, $10^6$ c.u.      | 18.75        | 26.77            | 18.75                                      | 26.77  |
| CL, $10^6$ c.u.         | 4.78         | 5.36             | 4.78                                       | 5.36   |
| K, $10^6$ c.u.          | 18.77        | 26.79            | 18.77                                      | 26.79  |
| Y, $10^6$ c.u.          | 7.3          | 8.95             | 8.11                                       | 9.95   |
| DDC, $10^6$ c.u.        | 26.07        | 35.74            | 26.88                                      | 36.74  |

## 5. CONCLUSION

The power factor of the FCAED, which determines its energy and electromagnetic compatibility, can be calculated after modeling the electric drive using MATLAB software or by using the components of the power balance, or by using THD values or current and voltage distortion coefficients. It is advisable to construct control characteristics (dependencies on rotational speed within a specified range for a specific load characteristic) of the consumed active power, efficiency coefficients, phase shift, THD, and power. For other loads in terms of value and nature, these characteristics will differ.

The criterion of discounted costs allows for a cost-based comparison of comparable FCAEDs to select the best option. It can be utilized in the development of new FCAEDs. Despite the significant cost of a matrix converter compared to a DC link converter (more than 10 times as expensive), the mid-range discounted costs decrease by more than 11 times for a drive with a matrix converter compared to a drive with a DC link converter, given the same specified payback period and annual inflation rate.

This criterion should take into account the costs to compensate not only for reactive power, determined by the phase shift coefficient between the fundamental harmonics of current and voltage, but also the costs to compensate for the distortion power caused by higher harmonics at the drive input. Since the phase shift coefficients in the considered drives have large values close to 1, there is no need for expenditure on reactive power compensation. But for the first time, it is proposed to include the costs of distortion power compensation, determining the electromagnetic compatibility of the drive, in the calculation of the range discounted criterion.

The calculation result of the discounted costs criterion is influenced by the load operating mode. In the examples considered, the discounted costs differ in the case of assigning the control range and in the case of assigning the tachogram. The discounted costs in the case of assigning the tachogram decrease by more than 10 times for a drive with a matrix converter compared to a drive with a DC link converter, given the

specified payback period and annual inflation rate. The discounted costs increase when inflation is considered. However, the cost ratio for FCAEDs with DC link and matrix converters remains practically unchanged.

## FUNDING INFORMATION

The publication fee was funded by the Berlin School of Economics and Law (HWR Berlin).

## AUTHOR CONTRIBUTIONS STATEMENT

This journal uses the Contributor Roles Taxonomy (CRediT) to recognize individual author contributions, reduce authorship disputes, and facilitate collaboration.

| Name of Author       | C | M | So | Va | Fo | I | R | D | O | E | Vi | Su | P | Fu |
|----------------------|---|---|----|----|----|---|---|---|---|---|----|----|---|----|
| Viktor Petrushyn     | ✓ | ✓ |    | ✓  |    | ✓ |   | ✓ |   | ✓ |    | ✓  | ✓ |    |
| Juriy Plotkin        |   | ✓ | ✓  |    | ✓  |   | ✓ |   | ✓ |   |    | ✓  |   | ✓  |
| Vasily Horoshko      | ✓ |   |    | ✓  | ✓  |   | ✓ |   | ✓ |   | ✓  |    |   |    |
| Rostyslav Yenoktaiev |   | ✓ | ✓  |    |    | ✓ |   | ✓ |   | ✓ |    | ✓  |   |    |
| Andrii Yakimets      |   | ✓ |    | ✓  | ✓  |   | ✓ |   |   | ✓ | ✓  |    |   |    |

C : Conceptualization

M : Methodology

So : Software

Va : Validation

Fo : Formal analysis

I : Investigation

R : Resources

D : Data Curation

O : Writing - Original Draft

E : Writing - Review & Editing

Vi : Visualization

Su : Supervision

P : Project administration

Fu : Funding acquisition

## CONFLICT OF INTEREST STATEMENT

Authors state no conflict of interest.

## DATA AVAILABILITY

The data that support the findings of this study are available from the corresponding author, [VP], upon reasonable request.




## REFERENCES

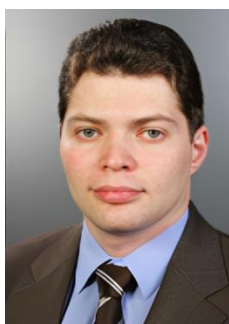
- [1] P. Szcześniak, *Three-Phase AC-AC Power Converters Based on Matrix Converter Topology*. in Power Systems. London: Springer London, 2013. doi: 10.1007/978-1-4471-4896-8.
- [2] A. Dasgupta and P. Sensarma, *Design and control of matrix converters*. in Energy Systems in Electrical Engineering. Singapore: Springer Singapore, 2017. doi: 10.1007/978-981-10-3831-0.
- [3] R. Alammari, Z. Aleem, A. Iqbal, and S. Winberg, "Matrix converters for electric power conversion: Review of topologies and basic control techniques," *International Transactions on Electrical Energy Systems*, vol. 29, no. 10, pp. 1–25, Oct. 2019, doi: 10.1002/2050-7038.12063.
- [4] P. Szczesniak, K. Urbanski, Z. Fedyczak, and K. Zawirski, "Comparative study of drive systems using vector-controlled PMSM fed by a matrix converter and a conventional frequency converter," *Turkish Journal of Electrical Engineering & Computer Sciences*, vol. 24, no. 3, pp. 1516–1531, 2016, doi: 10.3906/elk-1307-162.
- [5] R. K. Dubey, "A review paper on variable frequency drive," *Journal of Emerging Technologies and Innovative Research (JETIR)*, vol. 5, no. 6, pp. 207–210, 2018.
- [6] F. A. Samman, T. Waris, T. D. Anugerah, and M. N. Z. Mide, "Three-phase inverter using microcontroller for speed control application on induction motor," in *2014 Makassar International Conference on Electrical Engineering and Informatics (MICEEI)*, IEEE, Nov. 2014, pp. 28–32. doi: 10.1109/MICEEI.2014.7067304.
- [7] International Electrotechnical Commission, "IEC 60034-30-1:2014 Rotating electrical machines - Part 30-1: Efficiency classes of line operated AC motors (IE code)," 2014. [Online]. Available: <https://cdn.standards.iteh.ai/samples/19304/87264c341ee9453fabf58933851aa67a/IEC-60034-30-1-2014.pdf>
- [8] International Electrotechnical Commission, "IEC TS 60034-30-2:2016 Rotating electrical machines - Part 30-2: Efficiency classes of variable speed AC motors (IE-code)," 2016. [Online]. Available: <https://cdn.standards.iteh.ai/samples/21194/6a6c0777307c452bb1aee2f1db7a5f7c/IEC-TS-60034-30-2-2016.pdf>
- [9] V. Busher, S. Savich, S. Savich, and V. Medvediev, "Automated comparison of the technical and economic efficiency for crane mechanisms," *Eastern-European Journal of Enterprise Technologies*, vol. 2, no. 8(80), p. 37, Apr. 2016, doi: 10.15587/1729-4061.2016.66784.
- [10] R. Marino, P. Tomei, and C. M. Verrelli, *Induction Motor Control Design*. in Advances in Industrial Control. London: Springer London, 2010. doi: 10.1007/978-1-84996-284-1.




- [11] F. Tinazzi, M. Zigliotto, A. Boglietti, A. Cavagnino, and M. Cossale, "Energy efficiency assessment for inverter-fed induction motors," in *8th IET International Conference on Power Electronics, Machines and Drives (PEMD 2016)*, Institution of Engineering and Technology, 2016, pp. 6.-6. doi: 10.1049/cp.2016.0356.
- [12] M. N. Omar, M. M. Ismail, M. N. Ayob, and F. Arith, "Upgrading for overhead crane anti-sway method using variable frequency drive," *Bulletin of Electrical Engineering and Informatics*, vol. 11, no. 4, pp. 1837–1844, Aug. 2022, doi: 10.11591/eei.v11i4.3731.
- [13] J. Pyrhönen, T. Jokinen, and V. Hrabovcová, *Design of Rotating Electrical Machines*. Wiley, 2013. doi: 10.1002/9781118701591.
- [14] V. Petrushin, V. Vodichev, and R. Yenoktaiev, "Design criteria and range limits in the development of controlled induction motors," *International Journal on Electrical Engineering and Informatics*, vol. 11, no. 2, pp. 451–462, Jun. 2019, doi: 10.15676/ijeii.2019.11.2.15.
- [15] V. Petrushin, J. Plotkin, N. Almuratova, M. Mustafin, and M. Zharkymbekova, "Discounted costs range criterion modification for controlled asynchronous electric drives," *Energies*, vol. 16, no. 15, p. 5704, Jul. 2023, doi: 10.3390/en16155704.
- [16] A. B. Martínez, I. J. Navarro, V. S/ Santos, E. C. Quispe, and P. D. Donolo, "MATLAB/Simulink modeling of electric motors operating with harmonics and unbalance," *International Journal of Electrical and Computer Engineering (IJECE)*, vol. 12, no. 5, p. 4640, Oct. 2022, doi: 10.11591/ijece.v12i5.pp4640-4648.
- [17] R. D. Dole and P. V. Thakre, "Performance analysis of PI control based matrix converter for speed control of asynchronous motor using MATLAB/Simulink," in *2018 3rd International Conference on Communication and Electronics Systems (ICCES)*, IEEE, Oct. 2018, pp. 254–258. doi: 10.1109/CESYS.2018.8723886.
- [18] J. Vadillo, J. M. Echeverría, M. Martínez-Iturralde, and L. Fontán, "Modelling and simulation of indirect space vector modulated matrix converter using MATLAB®/Simulink®," *International Journal of Electronics*, vol. 96, no. 8, pp. 855–863, Aug. 2009, doi: 10.1080/00207210902860275.
- [19] MathWorks, "Three-phase matrix converter," MathWorks. Accessed: Oct. 06, 2024. [Online]. Available: <https://www.mathworks.com/help/sps/ug/three-phase-matrix-converter.html>.
- [20] H. Le-Huy, "Modeling and simulation of electrical drives using MATLAB/Simulink and Power System Blockset," in *IECON'01. 27th Annual Conference of the IEEE Industrial Electronics Society (Cat. No.37243)*, IEEE, pp. 1603–1611. doi: 10.1109/IECON.2001.975530.
- [21] R. W. De Doncker, D. W. J. Pulle, and A. Veltman, *Advanced electrical drives*. in Power Systems. Cham: Springer International Publishing, 2020. doi: 10.1007/978-3-030-48977-9.
- [22] S. Nadweh, N. Mohammed, O. Alshammari, and S. Mekhilef, "Topology design of variable speed drive systems for enhancing power quality in industrial grids," *Electric Power Systems Research*, vol. 238, p. 111114, Jan. 2025, doi: 10.1016/j.epr.2024.111114.
- [23] P. Dinolova, O. Dinolov, and V. Ruseva, "Experimental research on improving the energy efficiency of industrial-site induction motor drives," *E3S Web of Conferences*, vol. 638, p. 01016, Jul. 2025, doi: 10.1051/e3sconf/202563801016.
- [24] A. Hughes and B. Drury, *Electric motors and drives*. Elsevier, 2013. doi: 10.1016/C2011-0-07555-5.
- [25] International Electrotechnical Commission, "Electromagnetic compatibility (EMC) - Part 3-2: Limits - Limits for harmonic current emissions (equipment input current  $\leq 16$  A per phase) - (IEC 61000-3-2)," 2018. [Online]. Available: <https://cdn.standards.iteh.ai/samples/22247/bdec75030c3c4f82af83aa4fb86bb1d8/IEC-61000-3-2-2018.pdf>
- [26] International Electrotechnical Commission, "Electromagnetic Compatibility (EMC)—Limits for Harmonic Currents Produced by Equipment Connected to Public Low-Voltage Systems - (IEC 61000-3-12)," 2011. [Online]. Available: <https://cdn.standards.iteh.ai/samples/16966/85cef6616b0f4d06b7a86cfe3e60e808/IEC-61000-3-12-2011.pdf>

## BIOGRAPHIES OF AUTHORS






**Viktor Petrushyn**    received his Diploma degree in "Electric machines and apparatuses" at Odessa National Polytechnic University in 1968 and his Ph.D. in 1979. Since 1987, he has worked as an assistant professor at the Department of Electrical Machines of Odessa Polytechnic Institute. From 1993 to 1998, he was dean of the faculty of the electrification and automation industry. In 2002, he was habilitated and has worked since then as a professor of electrical machines at Odessa National Polytechnic University. He can be contacted at email: [viktor\\_petrushin@ukr.net](mailto:viktor_petrushin@ukr.net).






**Juriy Plotkin**    received his Diploma degree in electrical engineering/heavy current engineering at the University of Technology Berlin in 2002 and his Ph.D. in 2009, both with honors. Industrial background is based on work at Alstom Power Conversion in Berlin as a project engineer for rolling mill automation. From 2010 to 2012, he worked as a professor of renewable energy sources at Hamburg University of Applied Sciences. Since 2012, he has been a professor of electrical engineering/ energy technology at the Berlin School of Economics and Law. He can be contacted at email: [juriy.plotkin@hwr-berlin.de](mailto:juriy.plotkin@hwr-berlin.de).






**Vasily Horoshko**    received his master's degree in “Electromechanical automation system and electric drive” at Odesa Polytechnic National University in 2016 and his Ph.D. in 2020. Since 2019, he has been working as a research assistant and since 2021, a senior lecturer at the department of electromechanical of Odesa Polytechnic National University. He can be contacted at email: [vas.goroshko@gmail.com](mailto:vas.goroshko@gmail.com).



**Rostyslav Yenoktaiev**    received his master's degree in “Electric Machines and Apparatuses” from Odessa National Polytechnic University in 2015 and his Ph.D. in 2019. From 2016 to 2019, he worked as a research assistant, and from 2019, as a senior lecturer at the Department of Electrical Machines of Odessa National Polytechnic University. Since 2025, he has been working as a research associate at the Berlin School of Economics and Law. He can be contacted at email: [rostyslav.yenoktaiev@hwr-berlin.de](mailto:rostyslav.yenoktaiev@hwr-berlin.de).



**Andrii Yakimets**    received his Diploma degree in “Electric machines and apparatuses” at Odesa Polytechnic National University in 1998 and his Ph.D. in 2004. Since 2006, he has worked as an assistant professor at the Department of Electrical Machines of Odesa Polytechnic National University. From 2017 to 2021, he was the head of the chair of electrical machines. From 2022, he has worked as an associate professor of the chair of electromechanical engineering at Odesa Polytechnic National University. He can be contacted at email: [yakimets\\_andriy@ukr.net](mailto:yakimets_andriy@ukr.net).